Düzce University
Journal of Science & Technology

Research Article

An Experimental Effort on Impact Properties of Poly(lactic acid) Produced by Additive Manufacturing

Çağın BOLAT [a,*], Berkay ERGENE [b]

[a] *Faculty of Engineering, Samsun University, Samsun, TURKEY*
[b] *Faculty of Technology, Pamukkale University, Denizli, TURKEY*
* *Corresponding author's e-mail address: cagin.bolat@samsun.edu.tr*
DOI: 10.29130/dubited.1075259

ABSTRACT

Additive manufacturing (AM) has been highly popular in recent years and the number of scientific efforts on this useful manufacturing way has increased day by day. Up to now, the majority of the studies accumulated on the physical and mechanical properties of the three-dimensional (3D) printed specimens. In this paper, the impact properties of the additively manufactured poly(lactic acid) (PLA) parts were addressed in detail. All specimens were manufactured by way of fused deposition modeling (FDM). After the manufacturing, hardness and surface roughness measurements were carried out to probe the effectiveness of the offered FDM technique. In order to detect impact features of the PLA specimens, Charpy v-notch impact tests were conducted and the influence of the notch angle was examined. As for the manufacturing parameters, the factor of infill density was altered and its effects on the impact behaviors of the specimens were established. Furthermore, micro and macro damage analyses were performed elaboratively on tested PLA specimens to comprehend the main mechanism of deformation better.

Keywords: *Poly(lactic acid), Additive manufacturing, Infill density, Charpy notch test, Impact property*

Eklemeli İmalat ile Üretilen Poli(laktik asit)in Darbe Özellikleri Üzerine Deneysel Bir Çalışma

ÖZET

Eklemeli imalat (Eİ) yöntemleri son yıllarda oldukça popüler hale gelmiştir ve bu faydalı imalat yöntemine yönelik bilimsel çalışmaların sayısı her geçen gün artmıştır. Şimdiye kadar, çalışmaların çoğu, üç boyutlu (3B) basılmış numunelerin fiziksel ve mekanik özellikleri üzerine olmuştur. Bu yazıda, eklemeli olarak üretilen poli(laktik asit) (PLA) parçaların darbe özellikleri ayrıntılı olarak ele alınmıştır. Tüm numuneler, eriyik yığma modelleme yoluyla üretilmiştir. İmalattan sonra, önerilen tekniğin etkinliğini araştırmak için sertlik ve yüzey pürüzlülüğü ölçümleri yapılmıştır. PLA numunelerin darbe özelliklerini tespit etmek için Charpy v-çentik darbe testleri yapılmış ve çentik açısının etkisi incelenmiştir. İmalat parametrelerinde ise, dolgu yoğunluğu faktörü değiştirilmiş ve numunelerin darbe davranışları üzerindeki etkileri belirlenmiştir. Ayrıca, deformasyonun ana mekanizmasını daha iyi anlamak için test edilen PLA numuneleri üzerinde ayrıntılı bir şekilde mikro ve makro hasar analizleri yapılmıştır.

Anahtar Kelimeler: *Poli(laktik asit), Eklemeli imalat, Doluluk oranı, Charpy çentik testi, Darbe özelliği*

Received: 17/02/2022, Revised: 26/12/2022, Accepted: 10/01/2023

I. INTRODUCTION

Three-dimensional (3D) printing technology, which is also known as additive manufacturing (AM), is an effective and useful method to create well-defined solid parts. This methodology is not only used for rapid prototyping and but also is preferred in special applications like medical implants, tissue engineering, aerospace, and construction [1-3]. In comparison with traditional manufacturing routes such as machining, casting, plastic deformation, and welding, 3D printing technology can be interpreted as promising for lots of improvements both in the process developments and new material types, so the number of scientific efforts on this technology has increased in recent years. Usually, as base materials, acrylonitrile-butadiene-styrene (ABS), poly(lactic acid) (PLA), and poly(ethylene terephthalate glycol) (PETG) polymers are utilized by researchers and engineers working on prototyping or special-purpose manufacturing [4-10]. Apart from these widely-used polymers, aluminum-based alloys, magnesium-based alloys, some grades of steel, and titanium alloys can be produced by way of 3D printing [11, 12]. When the 3D printing methods are scanned in detail by analyzing the technical literature, it can be propounded that fundamental processes can be categorized into two different groups: fusion-assisted techniques (fused deposition modeling, selective laser melting, electron beam melting, and laser powder bed fusion), and non-fusion-assisted techniques (binder jet, material jet, and extrusion) [13]. Considering all of these methods, it can be expressed that the most chosen technique is fused deposition modeling (FDM) where different thermoplastic filaments were used. If the technique is looked at briefly, FDM-based 3D printer machines run by extruding thermoplastic polymer filaments via a pre-heated nozzle system. Then, melted filament material proceeds the path adjusted by the computer aided design (CAD) program to reach the final shape. Furthermore, it can be underlined that the FDM technique allows the setting of the mechanical and physical features by controlling the void/gap density, layer thickness, and filament building direction. Lastly, it was alleged that FDM technology is going to be one of the significant components of the four-dimensional (4D) printing technology which includes 3D printing of the smart materials [14].

Poly(lactic acid) (PLA) is a special kind of thermoplastic material and is derived from renewable resources like corn starch or sugar cane. In contrast to other plastics derived from the distillation and polymerization of nonrenewable petroleum reserves, PLA materials can be defined as bioplastics. Owing to their easy printability, PLA filaments have been consumed for a while by lots of polymer engineers and investigators in 3D printing applications. However, the majority of the researchers have piled up on the physical features, mechanical properties, and process optimization. In addition, efforts on the unknown points regarding the effects of the process parameters on the mechanical responses of the additively manufactured PLA parts have still continued. For instance, Deng et al. [15] manufactured PLA parts via the FDM technique and revealed that the tensile failure strength of the samples with the same printing angles was bigger as its layer thickness decreased. Fernandes et al. [16] tried to figure out the influences of the printing parameters on the tensile responses of the 3D printed PLA samples and pointed out that maximum ultimate tensile strength value was determined for the sample having 60% infill rate and 0.1 mm layer thickness. Khan et al. [17] conducted a series of mechanical tests on 3D printed PLA samples in order to find the impacts of the infill pattern on the tensile and flexural strength values. The research team noted that the rectilinear infill pattern was the best for this purpose. Nugroho et al. [18] analyzed the effects of the layer thickness on the flexural properties of 3D printed PLA samples and declared that the highest flexural strength was detected for the sample having the highest layer thickness of 0.5 mm. Hanon et al. [19] utilized the FDM method for PLA production and showed that FDM could lead to anisotropy in the products. Zhang et al. [20] predicted a model to ascertain tensile properties of additively manufactured PLA parts and reported that tensile strength of materials dropped as layer thickness increased. Pearce et al. [21] scrutinized the influence of color on the tensile responses of FDM-built PLA samples and put forward that the best results belonged to white-colored samples. Grasso et al. [22] focused on the thermo-mechanical features of the 3D printed PLA samples and alleged that as the test temperature went up ductility of the PLA samples also raised. Aside from these valuable works focusing on solely PLA, PLA-based composites have also been produced via the FDM method, and obtained parts have been tested by different investigators [23 - 28]. Camargo et al. [29] focused on the mechanical responses of FDM printed PLA/graphene parts and showed that impact energy decreased with rising infill ratio. Adam et al. [30] alleged that addition of carbon nano tubes improved impact properties of PLA. Ahmed et al. [31] produced hybrid carbon fiber added PLA/ABS samples and explained that damage structures of PLA and ABS laminas were different in terms of pore types. Kechagias et al. [32] worked on wood/PLA composites fabricated via FDM and they explored that layer thickness was the decisive factor for surface quality. In another work, Jafferson et al. [33] revealed that increasing wood ratio in PLA filament provided better impact properties. Thanks to these endeavors, composite prototypes can be evaluated in terms of physical, microstructural, and mechanical behaviors.

In this paper, contrary to frequently studied mechanical properties like yield strength, tensile strength, elastic modulus, elongation, and ductility, impact properties of the FDM-built PLA samples were examined elaborately by using Charpy v-notch test equipment. In this context, notch angles and infill density values of the PLA samples were changed and their influences were explored. Moreover, after-deformation inspections were carried out on macroscopic and microscopic scales so as to comprehend the failure mechanism of the samples in detail.

II. MATERIAL AND METHOD

In this experimental study, PLA filaments supplied from Microzey Limited Company were used. Table 1 given below shows some significant physical and mechanical properties of PLA filaments in accordance with the information of the supplier.

Table 1. *Physical and mechanical properties of PLA filament*

Diameter *(mm)*	**Color**	**Density** *(kg/m^3)*	**Bed temperature** *(°C)*	**Printing temperature** *(°C)*	**Elasticity modulus** *(MPa)*	**Tensile strength** *(MPa)*	**Elongation at break** *(%)*
1,75	White	1240	60-80	190-210	1500	50	7

As for the manufacturing stage, Ender Pro 3 model 3D printer was used and FDM principles were applied during the manufacturing. In Figure 1, a real view of the printer machine and supporting software interface can be seen in detail. Additionally, all adjusted printing parameters can be found in Table 2.

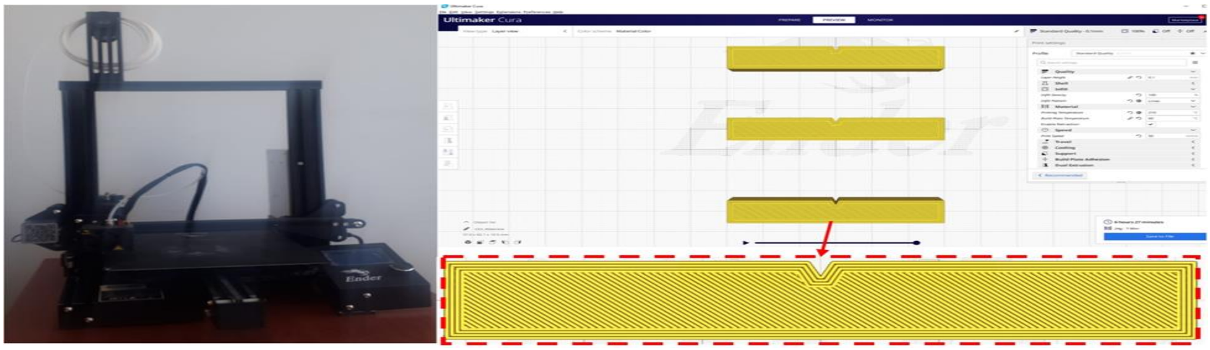

***Figure 1**. Real view of the 3D printer and slicing software interface*

Table 2. *FDM printing parameters*

Layer thickness *(mm)*	**Infill rate** *(%)*	**Infill type**	**Printing speed** *(mm/s)*	**Nozzle temperature** *(ºC)*	**Build plate temperature** *(ºC)*	**Raster angle** *(º)*	**Fan speed** *(%)*
0.1	40, 70, 100	Line	50	210	60	45/-45	100

Modified Charpy impact test specimens according to ASTM 6110 were designed in AutoCAD 2020 program, and then, created models having 63 mm length, 10 mm width and 10 mm height were saved as stl file. After that, the designed CAD files were transferred to the proper slicing program (Ultimaker Cura 4.4.1). Subsequently, attained G-code configuration from the slicing program was delivered to a 3D printer via an SD card. Finally, PLA impact test specimens were additively manufactured with a 3D printer. During the printing operation, no support structure was needed for the manufacturing process of specimens because of having no inclined surfaces. Besides, the production process was carried out in a room with ambient temperature of 25 °C. Following to the printing operations, all samples were categorized according to their altering notch angles and infill rates. In Figure 2 and Table 3, created product types can be seen.

Table 3. *3D printed Charpy impact test products*

Product	**Samples**	**Notch Angle** *(°)*	**Infill Rate** (%)
Type 1	1	30	40
	2	30	40
	3	30	40
Type 2	1	30	70
	2	30	70
	3	30	70
Type 3	1	30	100
	2	30	100
	3	30	100
Type 4	1	45	40
	2	45	40
	3	45	40
Type 5	1	45	70
	2	45	70
	3	45	70
Type 6	1	45	100
	2	45	100
	3	45	100
Type 7	1	60	40
	2	60	40
	3	60	40
Type 8	1	60	70
	2	60	70
	3	60	70
Type 9	1	60	100
	2	60	100
	3	60	100
Type 10	1	Unnotched	40

	2	Unnotched	40
	3	Unnotched	40
Type 11	1	Unnotched	70
	2	Unnotched	70
	3	Unnotched	70
Type 12	1	Unnotched	100
	2	Unnotched	100
	3	Unnotched	100

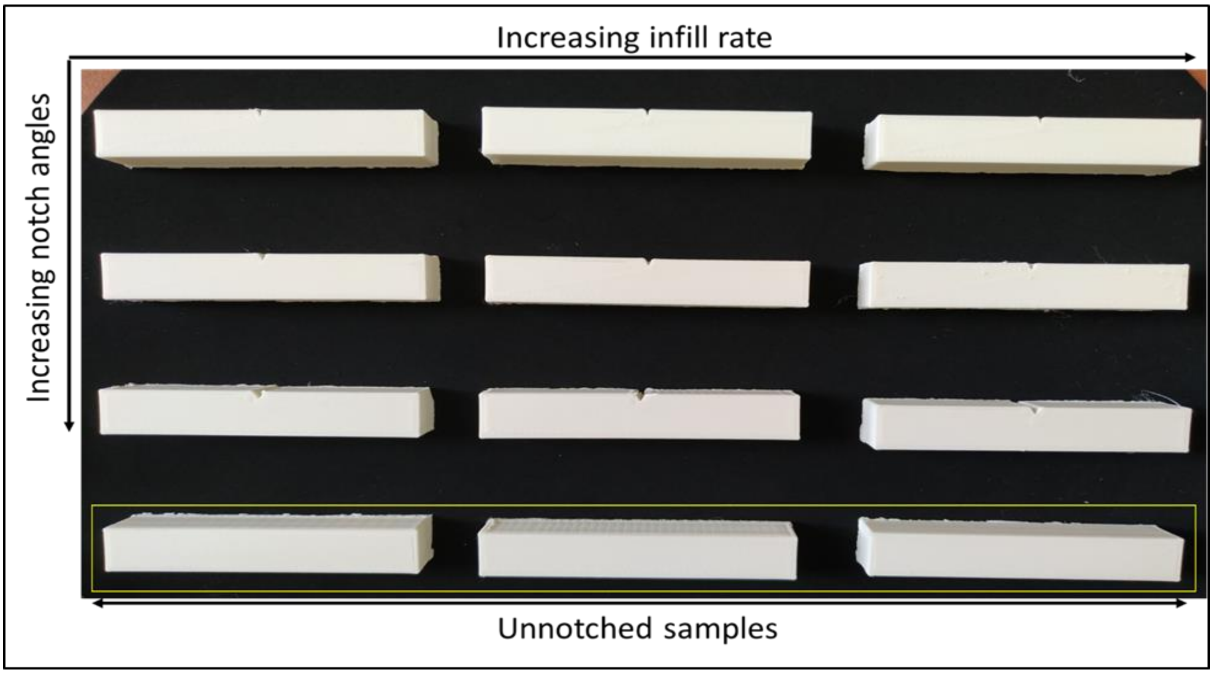

Figure 2. *FDM-built PLA impact test samples*

III. EXPERIMENTAL RESULTS

A. HARDNESS EVALUATIONS

In order to determine the hardness properties of the 3D printed PLA test specimens, Zwick & Co. Shore D test durometer was utilized. Test specimens with a length of 15 mm, a width of 15 mm, and a thickness of 10 mm were produced by using the same printing parameters. The dimensions of the hardness test specimen were determined according to ASTM D2240-15 standard that is a reference of hardness tests for polymer materials [34]. Figure 3 indicates the variation of hardness values depending on the changing infill rates.

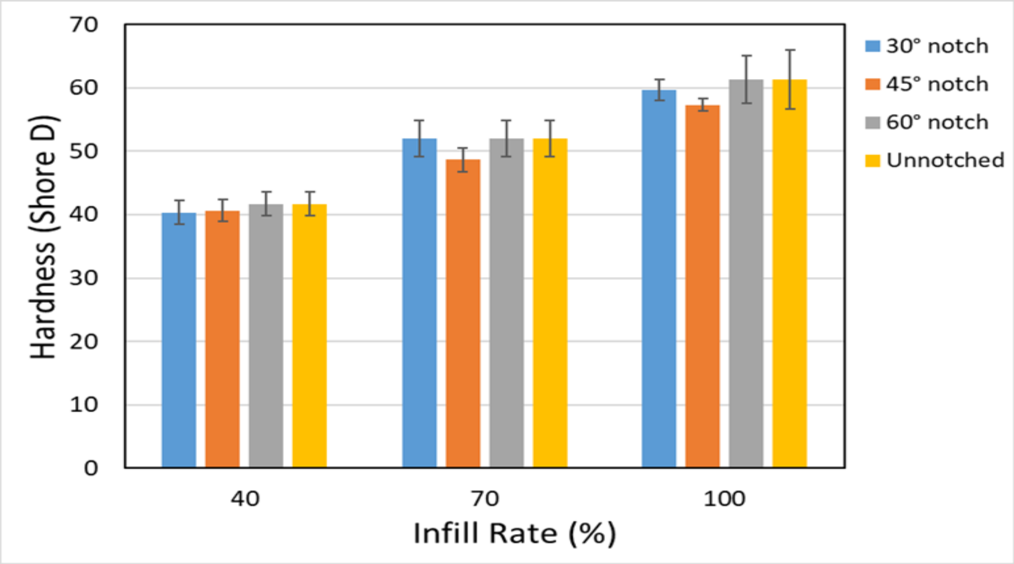

Figure 3. *Average hardness values of the impact samples depending on infill rates and notch angles*

According to the measured data, the highest hardness values of 68 Shore D (with the average of 61.3 Shore D) belonged to the sample having 100% infill rate. On the other hand, the lowest average hardness value of 40.3 Shore D was found for the sample having 40% infill rate. At this point, it can be alleged that as long as the infill rate levels increase, measured hardness values of the PLA samples also go up. This result can be attributed to the decreasing production gaps and good bonding strength of well-stacked layers in the samples having higher infill rates. In addition, similar upward trend of hardness values with increase of infill rates was reported in the study of Hsueh at al. [35] too. As for the samples possessing 70% infill rate, it is true to say that average hardness values of the manufactured samples varied between 52 Shore D and 48.7 Shore D. Besides, as predicted at the beginning of the measurements, there is not any direct interaction between the notch angles and hardness values.

B. SURFACE ROUGHNESS EVALUATIONS

Surface roughness measurements were conducted from five different locations on the top surface of the specimens by using Hommel Tester T500 model profilometer. Besides, an average value of five surface roughness measurement, which was performed perpendicular to the layers, was determined. In Figure 4, surface roughness measurement results can be seen. When the Figure 4 is examined, the decreasing trend of the average surface roughness values with an increase of infill rates is visible. What's more, average surface roughness values were measured as 6,3 μm, 5,8 μm and 5,1 μm respectively for the specimens manufactured with infill rates of 40%, 70% and 100%. Similar findings were also observed at other studies performed by Sammaiah et al. [36] and Dey and Yodo [37].

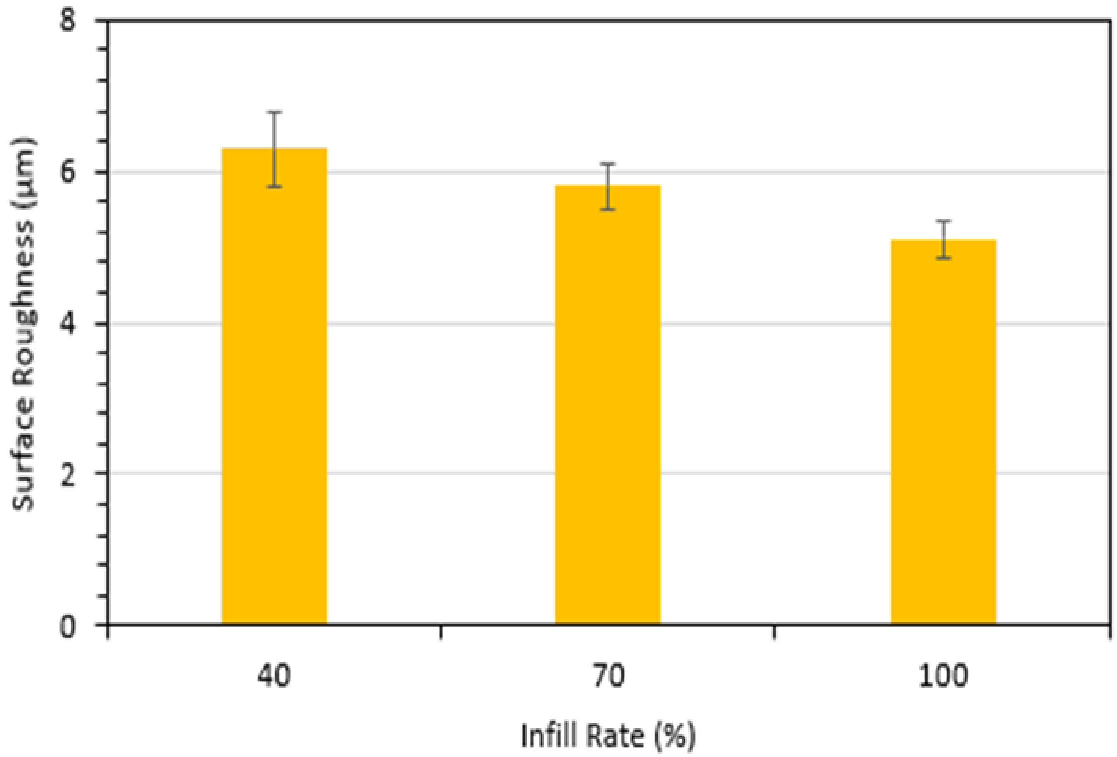

Figure 4. *Average surface roughness values depending on the infill rates*

C. IMPACT PROPERTIES

For determination of the impact properties of the 3D printed PLA samples, Charpy v-notch impact test procedures were applied. For this purpose, Devotrans Charpy tester was used and observed results were recorded simultaneously. Figure 5 demonstrates impact energy levels of the tested PLA samples depending on infill ratio and notch angles.

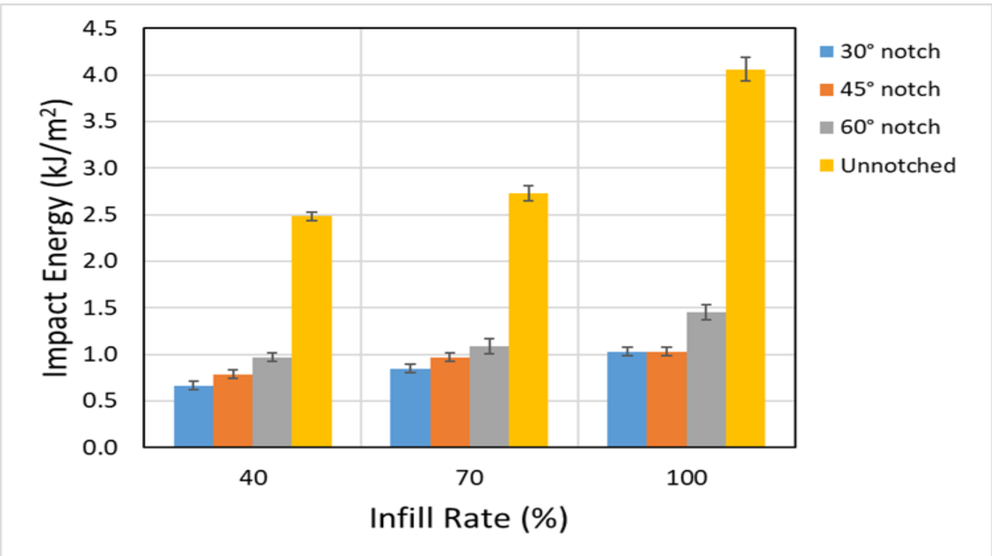

Figure 5. *Average impact energy values of the PLA samples depending on infill rates and notch angles*

From Figure 5, it is clear that there is a notably apparent notch sensitivity in the manufactured PLA samples and this situation directly influences the impact energy levels of the samples. As known from the knowledge of fracture mechanics, a stress localization is foreseen in the crack/notch tips and this circumstance was also observed in this study. According to the impact results, as the notch angle gets bigger, measured impact strength values rise due to diminishing stress concentration in the notch tip regions. On the other side, it can also be brought forward looking at Figure 5 that there is an affirmative relationship between the infill ratio values and impact properties. This outcome can be explained with the easy propagation of the impact cracks between the printing layers. The highest average impact energy value of 4.06 kJ/m^2 was seen for the sample possessing 100% infill rate and unnotched designed whereas the lowest average impact strength value of 0.67 kJ/m^2 was noted for the sample with 40% infill rate and 30° notch. For the samples having a 70% infill rate, similar trends were detected and the lowest average value of 0.85 kJ7m^2 and the highest average value of 2.73 kJ/m^2 was measured for the samples with a 40% infill rate/30° notch and with 100% infill rate/unnotched respectively. Similar to the observations recorded in this paper, Caminero et al. [38] performed a study on FDM PLA parts and reported that pure PLA part which produced with layer height of 0,12 mm in flat position exhibits 2,6 kJ/m^2. Furthermore, Tanveer et al. [39] focused on the effect of infill rate on impact properties of PLA part that manufactured with FDM technology. As a result of their study, they claimed that impact strength values go up with the increase of infill rates.

D. FAILURE ANALYSES

After the Charpy v-notch tests, damaged samples were inspected in terms of failure characteristics both in macroscopic and microscopic scales. During the macro analysis, visual inspections were done and evident damage modes that could be easily noticed at first glance were determined. On the other hand, Nikon SMZ 800 stereo microscope and DpxView software were used during the micro evaluations. In Figure 6 and Figure 7, macro and micro views of the damaged PLA samples with 30° notch angles can be seen depending upon changing infill rate values. Figure 6 shows that all samples exhibit deformation localization at notch tips and they completely break away. In addition, the fracture zones are not straight lines and have traverse deformation lines. This case can be explained by production gap distribution diversity and the gradient of bonding strength. From the point of microanalyses, Figure 7 indicates that damage distribution difference exists among the samples. Herein, it can be asserted that as the infill rate increase local damage sections become more apparent (Figure 7 (b) and Figure 7 (c)).

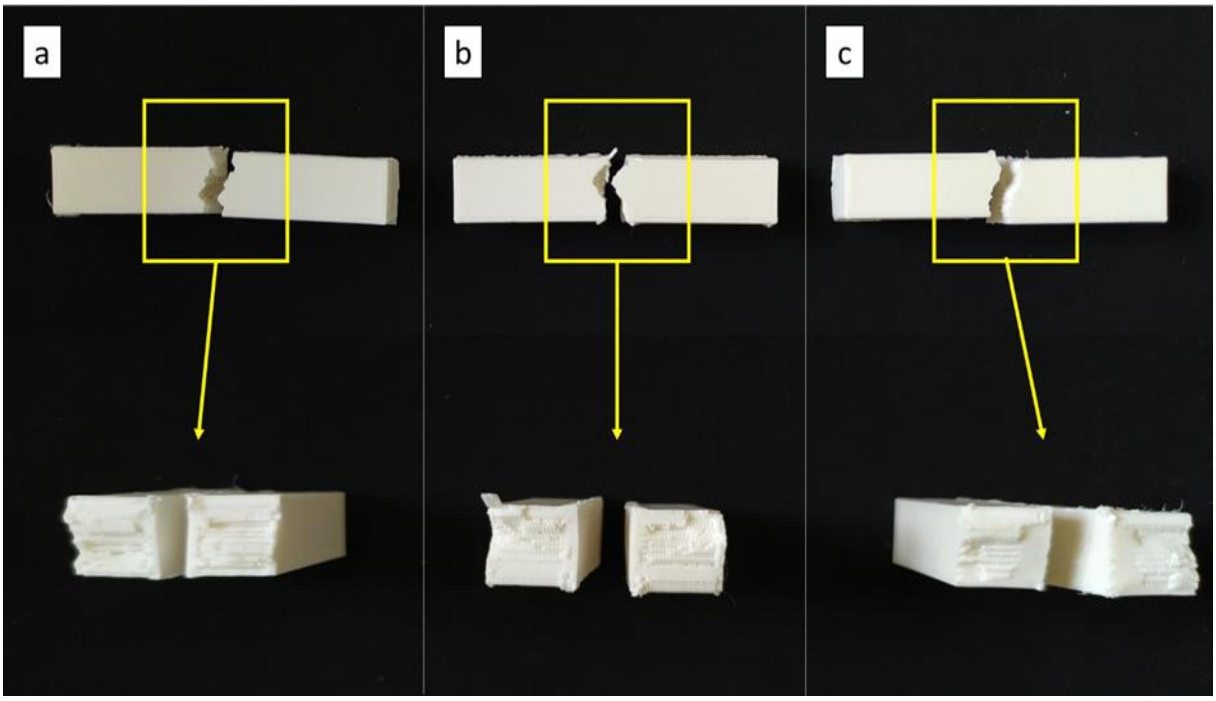

***Figure 6**. Macro views of the damaged samples with 30° notch angels: **(a)** 40% infill rate; **(b)** 70% infill rate; **(c)** 100% infill rate.*

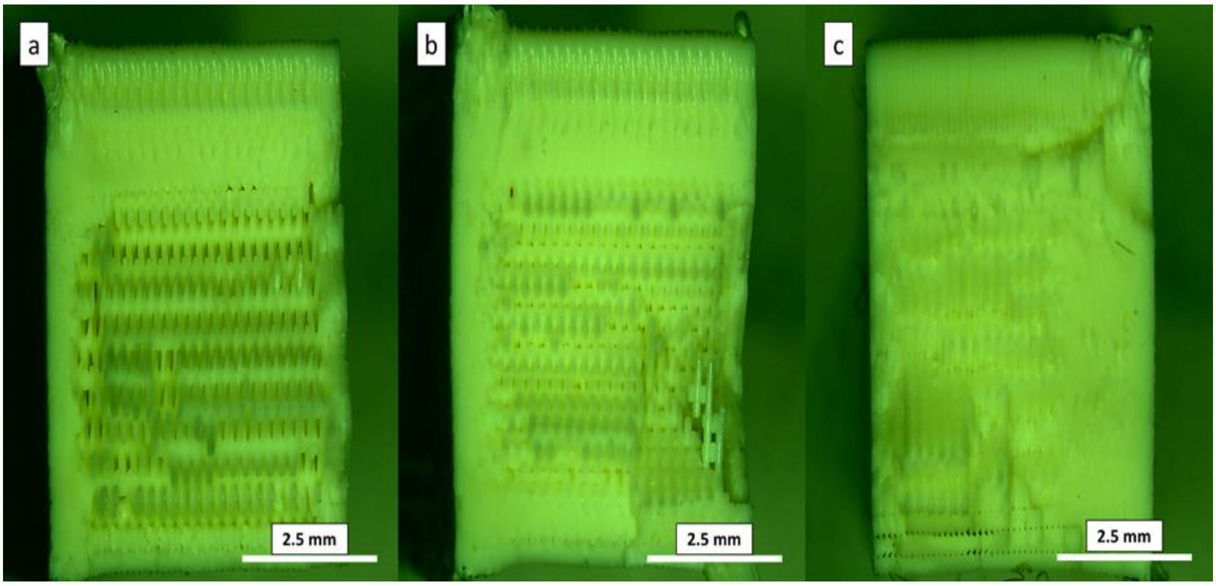

***Figure 7.** Micro views of the damaged samples with 30° notch angels: **(a)** 40% infill rate; **(b)** 70% infill rate; **(c)** 100% infill rate.*

In Figure 8 and Figure 9, macro and micro views of the deformed PLA samples with 45° notch angles can be looked at in relation to shifting infill rate values. From Figure 8, it can be expressed that traverse deformation lines are present in the samples having 40% (Figure 8 (a)) and 70% (Figure 8 (b)) infill rate values while a straight deformation line is realized for the sample having a 100% infill rate (Figure 8 (c)). This behavior might be stemmed from the presence of relatively homogeneous bonding strength in the sample with a 100% infill rate. Also, from the microanalyses, it is correct to claim that damage distribution difference exists among the samples as observed for the samples with 30° notch. Figure 9 demonstrates that cross-sectional damage distribution results are similar for 40% (Figure 9 (a)) and 70% (Figure 9 (b)) infill rate values but localized damage is seen if the infill rate is adjusted as 100% (Figure 9 (c)).

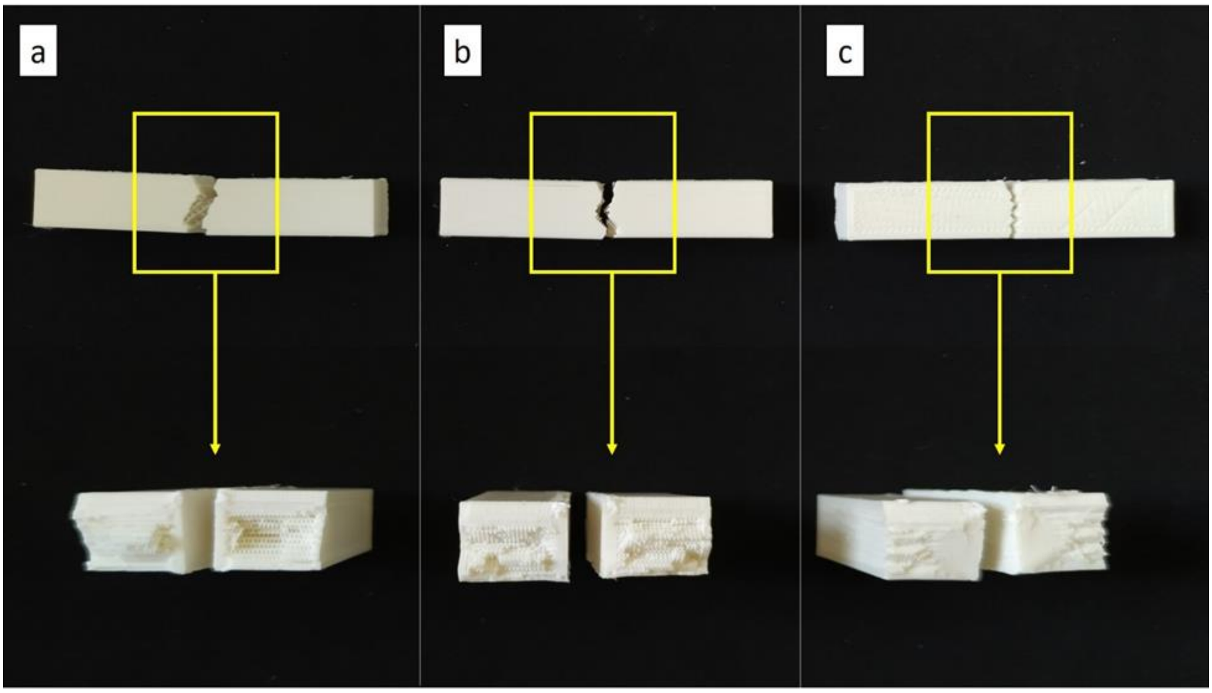

Figure 8. *Macro views of the damaged samples with 45° notch angels:* ***(a)*** *40% infill rate;* ***(b)*** *70% infill rate;* ***(c)*** *100% infill rate.*

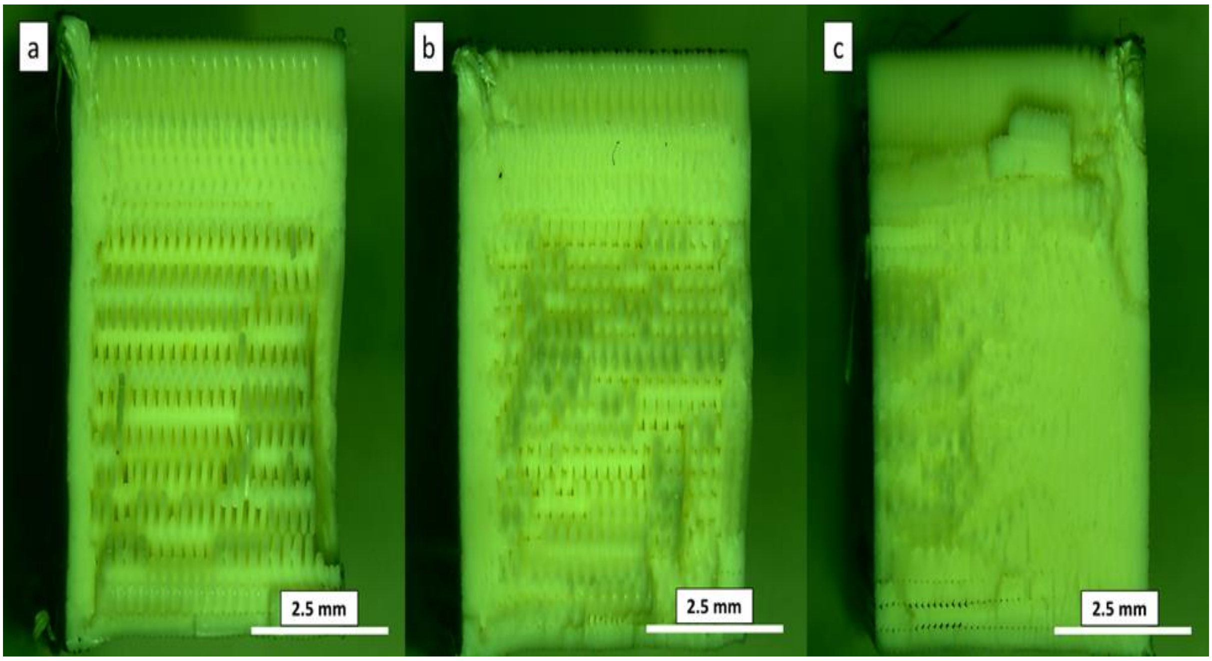

Figure 9. *Micro views of the damaged samples with 45° notch angels:* ***(a)*** *40% infill rate;* ***(b)*** *70% infill rate;* ***(c)*** *100% infill rate.*

In Figure 10 and Figure 11, macro and micro images of the damaged PLA samples with 60° notch angles can be examined in accordance with varying infill rate levels. Similar to the observed situation for other notch angles, randomly-existed and traverse-progressed deformation lines are ascertained for all samples with 60° notch angles (Figure 10 (a), Figure 10 (b), and Figure 10 (c)). Micro inspections depicted in Figure 11 (a), Figure 11 (b), and Figure 11 (c) point out that damage distribution difference decreases in the cross-sections of the tested samples owing to the increasing notch angle and decreasing stress concentration in the notch tips.

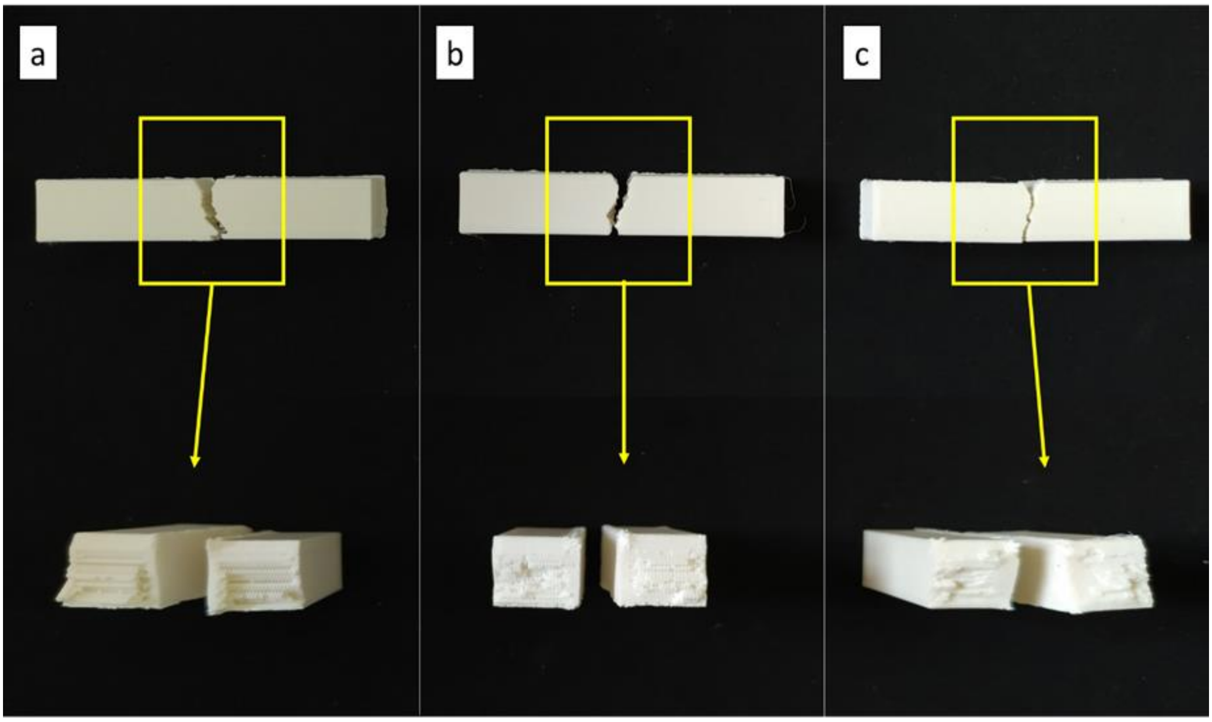

***Figure 10**. Macro views of the damaged samples with 60° notch angels: **(a)** 40% infill rate; **(b)** 70% infill rate; **(c)** 100% infill rate.*

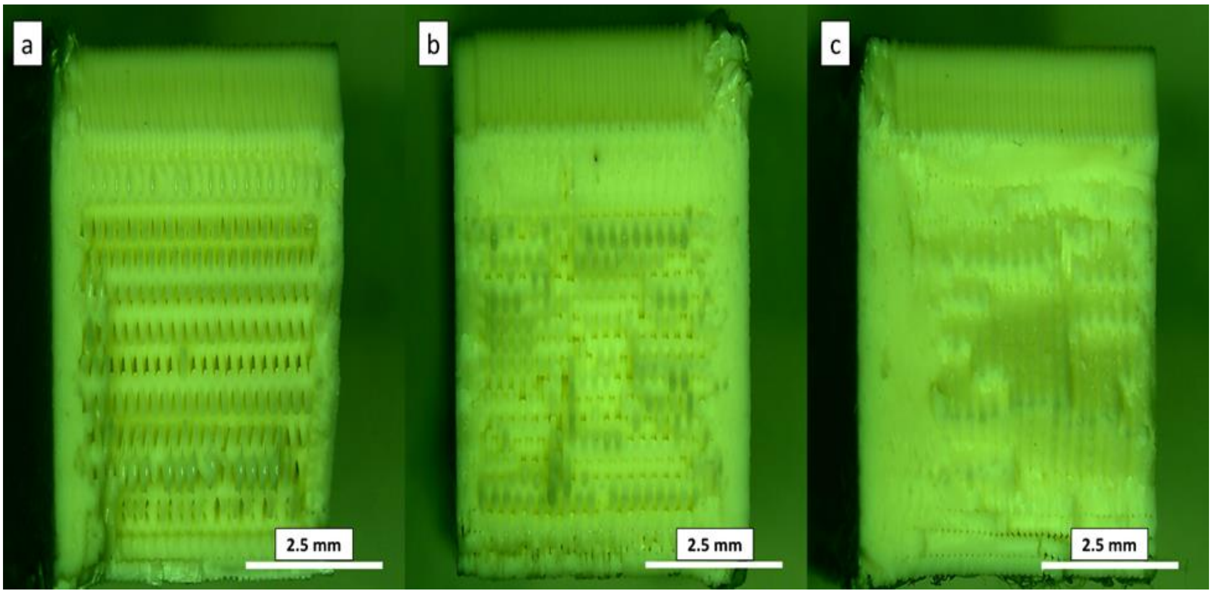

***Figure 11.** Micro views of the damaged samples with 60° notch angels: **(a)** 40% infill rate; **(b)** 70% infill rate; **(b)**100% infill rate.*

If the damage modes of the unnotched PLA samples are addressed, it is clear that there is not a direct relationship between the infill rate and damage styles of the samples. For instance, the samples with 40% (Figure 12 (a)) and 100% (Figure 12 (c)) infill rates show relatively straight deformation lines while the sample with 70% (Figure 12 (b)) infill rate carries a ragged deformation line. This observation can be explicated with nonexistance of the notch factor triggering the stress concentration, and the unbalanced distribution of production gaps. Looking at the micro observations illustrated in Figure 13, it is correct to emphasize that the destructive influence of the test hammer disperses to the whole impact area for all samples as a result of lacking a notch factor.

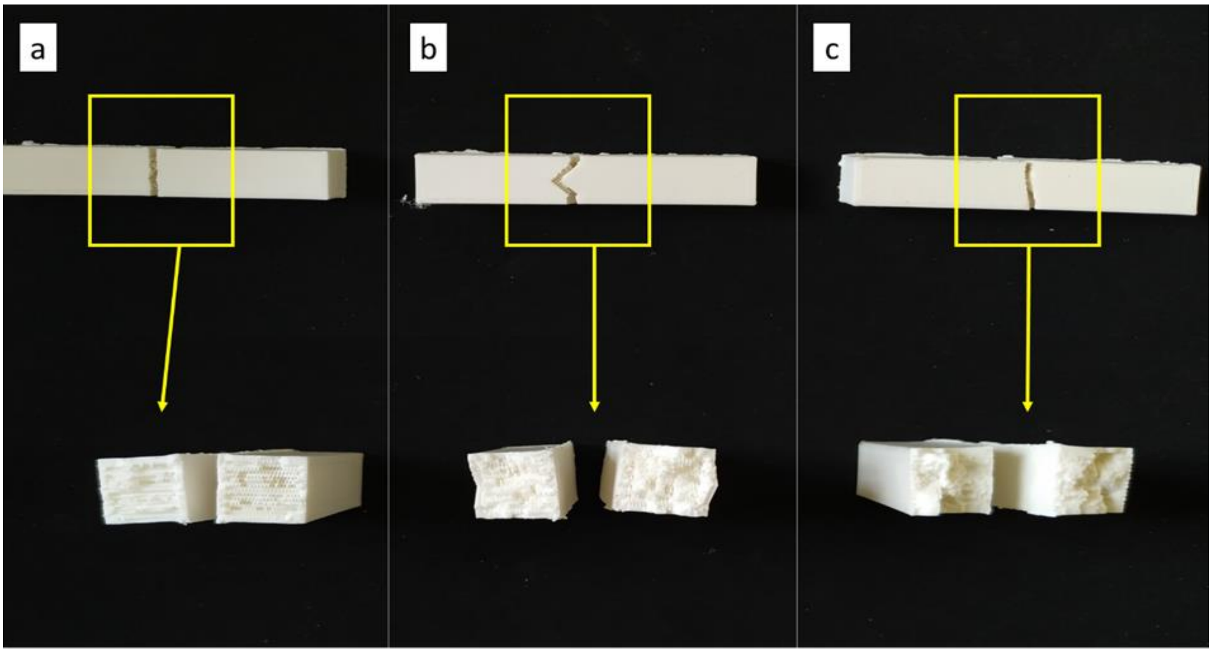

Figure 12. *Macro views of the damaged unnotched samples:* ***(a)*** *40% infill rate;* ***(b)*** *70% infill rate;* ***(c)****100% infill rate.*

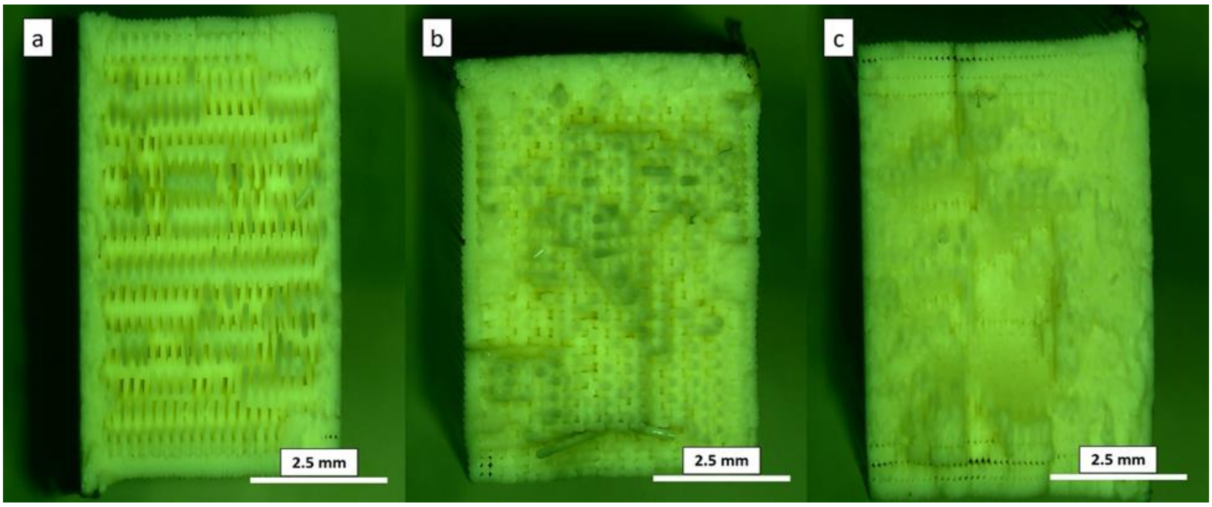

Figure 13. *Micro views of the damaged unnotched samples:* ***(a)*** *40% infill rate;* ***(b)*** *70% infill rate;* ***(c)*** *100% infill rate.*

IV. CONCLUSION

From this experimental study that focused on impact behavior of 3D printed PLA samples, the following major findings were obtained.

- FDM methodology is an effective way for manufacturing PLA samples having various different geometries and shapes. In this paper, the possibility of the production of lots of PLA samples with unlike notch angles was indicated.
- According to the measured data, the highest average hardness values of 61.3 Shore D belonged to the sample having 100% infill rate. On the other hand, the lowest average hardness value of 40.3 Shore D was found for the sample having 40% infill rate.

- Surface roughness of the samples was observed in a decreasing trend with an increase in infill rate values. Maximum and minimum average surface roughness values were determined as 6,3 µm and 5.1 µm for samples with infill rate of 40% and 100%.
- Impact tests showed that as the fill rate values of the samples increased, impact energy values also escalated. Furthermore, it was an affirmative relationship between the notch angle values and impact energy values.
- Following the macro damage analyses, it was seen that traverse deformation lines were the dominant mechanism although some of the samples had straight deformation lines due to production gaps.
- From the micro damage analyses, it was observed that all samples possessing 40% infill rates were subjected to cross-sectional deformation. However, samples with 70% and 100% showed local deformation zones for 30° and 45° notch angles but this circumstance changed with unnotched structure and increasing notch angles.

ACKNOWLEDGEMENT: As authors, we would like to thank the mechanical experiment laboratory staff in the Istanbul Technical University Faculty of Mechanical Engineering.

V. REFERENCES

[1] Q. Yan, H. Dong, J. Su, J. Han, B. Song, Q. Wei and Y. Shi, "A review of 3D printing technology for medical applications," *Engineering*, vol. 4, pp. 729–742, 2018.

[2] N. Shahrubudin, T.C. Lee, and R. Ramlan, "An overview on 3D printing technology: Technological, materials, and applications," *Procedia Manufacturing*, vol. 35, pp. 1286–1296, 2019.

[3] B. Yalçın and B. Ergene, "Metallurgy and method of new trend 3-D additive manufacturing in industry," *International Journal of Technological Sciences*, vol. 9, pp. 65–88, 2017.

[4] S. Wojtyła, P. Klama, and T. Tomasz Baran, "Is 3D printing safe? Analysis of the thermal treatment of thermoplastics: ABS, PLA, PET, and nylon," *Journal of Occupational and Environmental Hygiene*, 2017, vol. 14, pp. 80–85, 2017.

[5] J. Pizzicannella, F. Diomede, A. Gugliandolo, L. Chiricosta, P. Bramanti, I. Merciaro, T. Orsini, E. Mazzon, and O. Trubiani, "3D printing PLA/Gingival stem Cells/ EVs upregulate miR-2861 and -210 during osteoangiogenesis commitment," *International Journal of Molecular Sciences*, 2019, vol. 20, pp. 3256, 2019.

[6] T. Hanemann, D. Syperek, and D. Nötzel, "3D printing of ABS barium ferrite composites," *Materials*, vol. 13, pp. 1481, 2020.

[7] A. La Gala, R. Fiorio, M. Erkoç, L. Cardon, and D.R. D'hooge, "Theoretical evaluation of the melting efficiency for the single-screw micro-extrusion process: The case of 3D printing of ABS," *Processes*, vol. 8, pp. 1522, 2020.

[8] B. Ergene, İ. Şekeroğlu, Ç. Bolat, and B. Yalçın, "An experimental investigation on mechanical erformances of 3D printed lightweight ABS pipes with different cellular wall thickness," *Journal of Mechanical Engineering and Sciences*, vol. 15, pp. 8169–8177, 2021.

[9] S. Karabeyoğlu, B. Ergene, and Ç. Bolat, "An experimental study on wear performance of electrolytic multilayer Cu-Ni-Cr coated ABS under different test forces," *El-Cezeri Journal of Science*

and Engineering, vol. 8, pp. 666–674, 2021.

[10] N. Vidakis, M. Petousis, E. Velidakis, M. Liebscher, V. Mechtcherine, and L. Tzounis, “On the strain rate sensitivity of fused filament fabrication (FFF) processed PLA, ABS, PETG, PA6, and PP thermoplastic polymers,” *Polymers*, vol. 12, pp. 2924, 2020.

[11] M. Gupta, “3D printing of metals,” *Metals*, vol. 7, pp. 403, 2017.

[12] S.L. Sing, C.F. Tey, J.H.K. Tan, S. Huang, and W. Yee Yeong, *2 - 3D printing of metals in rapid prototyping of biomaterials: Techniques in additive manufacturing*, iind ed., United Kingdom: Woodhead Publishing, 2020, pp. 17-40.

[13] A. Mostafaei, A. Elliott, J.E. Barnes, F. Li, W. Tan, C.L. Cramer, P. Nandwana, and M. Chmielus, “Binder jet 3D printing—Process parameters, materials, properties, modeling, and challenges,” *Progress in Materials Science*, vol. 119, pp. 100707, 2021.

[14] B. Ergene, and B. Yalçın, “Investigation of 4D printing technology and application areas,” *International Journal of Technological Sciences*, vol. 12, pp. 108–117, 2020.

[15] T. Yao, J. Ye, Z. Deng, K. Zhang, Y. Ma, and H. Ouyang, “Tensile failure strength and separation angle of FDM 3D printing PLA material: Experimental and theoretical analyses,” *Composites Part B: Engineering*, vol. 188, pp. 107894, 2020.

[16] J. Fernandes, A.M. Deus, L. Reis, M.F. Vaz, and M. Leite, “Study of the influence of 3D printing parameters on the mechanical properties of PLA” in *3rd International Conference on Progress in Additive Manufacturing*, 2018, pp. 547-552.

[17] S.F. Khan, H. Zakaria, Y.L. Chong, and M.A.M. Saad, “Effect of infill on tensile and flexural strength of 3D printed PLA parts,” *IOP Conference Series: Material Science and Engineering*, vol. 429, pp. 012101, 2018.

[18] A. Nugroho, A. Ardiansyah, L. Rusita, and L. Larasati, “Effect of layer thickness on flexural properties of PLA (PolyLactid Acid) by 3D printing,” *Journal of Physics: Conference Series*, vol. 1130, pp. 012017, 2018.

[19] M.M. Hanon, R. Marczis, and L. Zsidai, “Influence of the 3D printing process settings on tensile strength of PLA and HT-PLA,” *Periodica Polytechnica Mechanical Engineering*, vol. 65, pp. 38–46, 2021.

[20] T. Yao, Z. Deng, K. Zhang, S. Li, “A method to predict the ultimate tensile strength of 3D printing polylactic acid (PLA) materials with different printing orientations,” *Composites Part B: Engineering*, vol. 163, pp. 393–402, 2019.

[21] B. Wittbrodt, and J.M. Pearce, “The effects of PLA color on material properties of 3-D printed components,” *Additive Manufacturing*, vol. 8, pp. 110–116, 2015.

[22] M. Grasso, L. Azzouz, P. Ruiz-Hincapie, M. Zarrelli, and G. Ren, “Effect of temperature on the mechanical properties of 3D-printed PLA tensile specimens,” *Rapid Prototyping Journal*, vol. 24, pp. 1337–1346, 2018.

[23] K.K. Guduru, and G. Srinivasu, “Effect of post treatment on tensile properties of carbon reinforced PLA composite by 3D printing,” *Materials Today: Proceedings*, vol. 33, pp. 5403–5407, 2020.

[24] H. Dou, Y. Cheng, W. Ye, D. Zhang, J. Li, Z. Miao, and S. Rudykh, “Effect of process

parameters on tensile mechanical properties of 3D printing continuous carbon fiber-reinforced PLA composites," *Materials*, vol. 13, pp. 3850, 2020.

[25] J.V. Ecker, A. Haider, I. Burzic, A. Huber, G. Eder, and S. Hild, "Mechanical properties and water absorption behaviour of PLA and PLA/wood composites prepared by 3D printing and injection moulding," *Rapid Prototyping Journal*, vol. 25, pp. 672–678, 2019.

[26] M. Ajay Kumar, M.S. Khan, and S.B. Mishra, "Effect of fused deposition machine parameters on tensile strength of printed carbon fiber reinforced PLA thermoplastics," *Materials Today: Proceedings*, vol. 27, pp. 1505–1510, 2020.

[27] A. Rahimizadeh, J. Kalman, R. Henri, K. Fayazbakhsh, and L. Lessard, "Recycled glass fiber composites from wind turbine waste for 3D printing feedstock: Effects of fiber content and interface on mechanical performance," *Materials*, vol. 12, pp. 3929, 2019.

[28] Y. Wang, M. Lei, and Q. Wei, "3D printing biocompatible L-Arg/GNPs/PLA nanocomposites with enhanced mechanical property and thermal stability," *Journal of Material Science*, vol. 55, pp. 5064–5078, 2020.

[29] J.C. Camargo, A.R. Machado, E.C. Almeida and E.F.M.S. Silva, "Mechanical properties of PLA-graphene filament for FDM 3D printing," *The International Journal of Advanced Manufacturing Technology*, vol. 103, pp. 2423–2443, 2019.

[30] B. Adam, and Z. Weltsch, "Thermal and Mechanical Assessment of PLA-SEBS and PLA-SEBS-CNT Biopolymer Blends for 3D Printing," *Applied Sciences*, vol. 11, pp. 6218, 2021.

[31] H. Ahmed, G. Hussain, S. Gohar, A. Ali, and M. Alkahtani, "Impact Toughness of Hybrid Carbon Fiber-PLA/ABS Laminar Composite Produced through Fused Filament Fabrication," *Polymers*, vol. 13, pp. 3057, 2021.

[32] D. Chaidas, and J.D. Kechagias, "An investigation of PLA/W parts quality fabricated by FFF," *Materials and Manufacturing Processes*, vol. 37, pp. 582–590, 2022.

[33] D. Deb, and J.M. Jafferson, "Natural fibers reinforced FDM 3D printing filaments," *Materials Today Proceedings*, vol. 46, pp. 1308–1318, 2021.

[34] *Standard test method for rubber property-durometer hardness*, ASTM D2240-15e1, 2015.

[35] M.H. Hsueh, C.J. Lai, K.Y. Liu, C.F. Chung, S.H. Wang, C.Y. Pan, W.C. Huang, C.H. Hsieh, and Y.S. Zeng, "Effects of printing temperature and filling percentage on the mechanical behavior of fused deposition molding technology components for 3D printing," *Polymers*, vol. 13, pp. 2910, 2021.

[36] P. Sammaiah, K. Rushmamanisha, N. Praveenadevi, and I.R. Reddy, "The influence of process parameters on the surface roughness of the 3D printed part in FDM process," *IOP Conference Series: Materials Science and Engineering*, vol. 981, pp. 042021, 2020.

[37] A. Dey, and N. Yodo, "A systematic survey of FDM process parameter optimization and their influence on part characteristics," *Journal of Manufacturing and Materials Processing*, vol. 3, pp. 64, 2019.

[38] M.A. Caminero, J.M. Chacon, E. García-Plaza, P.J. Nunez, J.M. Reverte, and J.P. Becar, "Additive manufacturing of PLA-based composites using fused filament fabrication: Effect of graphene nanoplatelet reinforcement on mechanical properties, dimensional accuracy and texture," *Polymers*, vol. 11, pp. 799, 2019.

[39] M.Q. Tanveer, A. Haleem, and M. Suhaib, "Effect of variable infill density on mechanical behaviour of 3-D printed PLA specimen: an experimental investigation," *SN Applied Sciences*, vol. 1, pp. 1701, 2019.